RESEARCH PAPER

Dual-component stearoyl polyoxyl-32 glyceride clay composites for enhanced curcumin solubility, stability, and antimicrobial activity.

Prashant B. Gurav[1,2]*, Chetan M. Detroja[1]

[1] Department of Pharmaceutics, School of Pharmacy, RK University, Rajkot 360001, Gujarat, India
[2] Department of Pharmaceutics, Indira Institute of Pharmacy, Sadavali, Ratnagiri 415804, Maharashtra, India.
Address for correspondence
prashantpharma.1980@gmail.com
0000-0002-8319-6330

ABSTRACT:

This research developed a polyoxylglycerides based solubilization system by combining a curcumin-Gelucire® 50/13 dispersion within a gellan gum-montmorillonite clay matrix. Dual-component composites were prepared in three clay: polymer ratios (1:1, 1:2, 1:3) using solvent dispersion and evaporation. Phase solubility studies identified the optimum curcumin: Gelucire® 50/13 ratio as 1:9.6, further supported by molecular docking. The 1:1 formulation (NCGC1) was examined through release profiling, with results validated by FTIR, TGA, DSC, and SEM-EDX. Antimicrobial activity was assessed by well-diffusion. Phase solubility showed more negative Gibbs free energy and Ks ≈ 1.286, indicating higher-order complexation, consistent with docking. Release studies of NCGC1 showed >90% curcumin release, attributed to Gelucire® micellization and gellan gum swelling. pH stability confirmed reduced degradation at pH 8 (15.57% vs. 36.98% for free curcumin). SEM-EDX revealed increased carbon (47.64%) and oxygen (38.68%) with suppressed silicon (10.50%) and aluminum (2.52%), confirming organic incorporation. Characterization indicated curcumin excipient compatibility and amorphous dispersion within the clay matrix. NCGC1 also exhibited significant antimicrobial activity compared to aqueous curcumin suspension. Thus, reciprocal use of Gelucire® 50/13 and gellan gum-montmorillonite composites enhanced curcumin's solubility, stability, and antimicrobial potential.

Keywords: Curcumin, Gelucire®, montmorillonite, Solubility, Antimicrobial.

INTRODUCTION

Curcumin, a yellow-colored extract derived from the turmeric rhizome (Curcuma longa), has been a staple of traditional medicine for centuries. It is the primary and most extensively studied compound among the curcuminoids, a group of dimeric derivatives of ferulic acid commonly found in Indian cuisine [1]. Beyond its use as a food coloring additive, curcumin has gained significant attention for its wide range of medicinal qualities, particularly antioxidant, antimicrobial, and anti-inflammatory effects [2,3]. Although curcumin exhibits diverse pharmacological activities, its clinical application is hindered by poor water solubility (3.12 mg/L at 25 °C) and hydrophobicity [4]. This results in low bioavailability, poor absorption in systemic circulation, and limited tissue distribution. Serum concentrations rarely exceed 60 nmol/L, and curcumin further suffers from photosensitivity and chemical instability during manufacturing and storage [5]. Reports indicate that nearly 90% of curcumin decomposes within 30 minutes at physiological pH 7.4, underscoring the need for effective stabilization strategies [6,7].

Various formulation approaches including nanoparticles, liposomes, micelles, and polymeric carriers have been explored to overcome these limitations [8-11]. Polyoxylglycerides such as Gelucire® 50/13 (GL) are amphiphilic excipients with high hydrophilic-lipophilic balance (HLB), widely utilized in self-emulsifying and supersaturating drug delivery systems to improve the bioavailability of poorly soluble drugs [12-15]. These semicrystalline carriers, classified as GRAS, are composed of polyethylene glycol esters of long-chain fatty acids and glycerides, and their proven utility in lipid-based formulations makes them attractive candidates for curcumin delivery [16]. Gellan gum (GG), an anionic microbial polysaccharide produced by *Sphingomonas elodea*, is widely recognized for its biocompatibility, biodegradability, and strong gel-forming ability. It has been extensively applied in drug delivery systems to provide sustained release,

mucoadhesion, and stabilization of labile bioactives. Recent reviews highlight its versatility in formulations such as hydrogels, microparticles, nanoparticles, and films [17].

Montmorillonite (MT) a natural clay mineral and major component of bentonite, having exceptional swelling capacity, high adsorption potential, and excellent biocompatibility. Recent studies highlight its ability to improve solubility, dissolution rate, and bioavailability of poorly water-soluble drugs in polymeric nanocomposites [18].

Despite extensive efforts, curcumin poor solubility and instability remain major barriers to get stable formulation option. Polyoxylglycerides such as GL provide lipid-based solubilization, while natural polymers like GG and layered silicates such as MT offer complementary stabilization through hydrogel entrapment and interlayer adsorption. Building on these advances, the present study investigates a dual component system in which curcumin is dispersed within GL and encapsulated in a GG-MT composite matrix. This hybrid design aims to achieve enhanced solubility, improved pH stability, and antimicrobial activity, thereby establishing a multifunctional and scalable drug delivery platform for oral as well as topical administration of curcumin.

MATERIAL AND METHODS

Material

Curcumin, MT, and GG were purchased from Sigma Aldrich, and GL was a kind gift sample from Gattefosse France. All other reagents, solvents, and chemicals were of analytical grade and purchased locally.

Methods

Phase solubility

To investigate the complexation behaviour and solubility enhancement of the drug, a phase solubility study was conducted. In this a surplus amount of curcumin was added into glass vials each having 10 mL of distilled water (DW) with varying concentrations of GL (0%, 0.25%, 0.5%, 0.75%, 1.0%, 1.25%, and 1.5%w/v) respectively, blended for 15 min by vortex mixer. Then screw-caped vials were shaken for 24 h on a mini rotary shaker at room temperature. After due course of time the samples were filtered using 0.45µ membrane filter [19, 20]. The resulting filtrate was suitably diluted and analysed using a UV-Visible spectrophotometer (Shimadzu UV-1900i) at a wavelength of 423 nm. The Gibbs free energy (ΔG) and stability constant (Ks) were determined based on the equations presented below

$$\Delta G_0 = -2.303RTLog\frac{S_0}{S_1}\text{.....1}$$

Where,

G, ideal gas constant, T = absolute temperature (Kelvin),

So, solubility of curcumin in various strengths of GL,

Ss, solubility of curcumin in aqueous medium.

Binding or stability constant (Ks) was computed by using bellow equation,

$$K_s = \frac{Slope}{S_0} \times (1 - Slope)\text{.....2}$$

Where,

So, is the solubility of curcumin without GL.

Conformational analysis by molecular modeling

The conformational characterization of curcumin and GL complexation during dispersions was guided using a computer-aided molecular modeling technique. ChemDraw Ultra 11.0 (Cambridge Soft, Cambridge, MA 02140, USA) was used for drawing the chemical structures, while Schrodinger Maestro 13.4 was used to create 3D molecular models. Docking in the program allowed for the structural preparation of the Curcumin-GL complex [21].

Preparation dual component system of Curcumin-GL-GG- MT clay-composite

Clay-composites were prepared by the solvent dispersion and evaporation method with slight modification to the reported work [22]. In the first step, prepared a dispersion of GG:MT (1:1) briefly, GG (250 mg) was dissolved in 25 mL DW, and on the other hand, MT (250 mg) was suspended in DW (50 mL) and stirred at 500 rpm using a magnetic stirrer for 1 h. Later, both mixtures were mixed and further stirred for 1 h at room temperature to produce a blend. In the second step, curcumin (50 mg) was added to priorly dissolved 480 mg GL in 65 mL of DW. Further, the mixture was bath sonicated for 1 h. Later, the resulting mixture was dispersed in the developed blend and stirred continuously for 2 h at 500 rpm to get solvent dispersion of clay composite (slurry). At the

end, the solvent was evaporated using hot air oven at 60 °C for 4 h to remove the solvent. The resulting dual component system consisting of curcumin:GL-GG:MT as composite and denoted as NCGC1. The different clay composites were prepared using MT: GG in the ratio of 2:1 (NCGC2), and 3:1 (NCGC3); by keeping curcumin: GL of 1:9.6 weight ratio constant (presented in Table 1).

Table 1: Different composition summary of curcumin clay-composites

Ingredients	NCGC1	NCGC2	NCGC3
MT (mg)	250	500	750
GG (mg)	250	250	250
Curcumin (mg)	50	50	50
GL (mg)	480	480	480

Curcumin content estimation

To quantify curcumin content in the clay-composites (NCGC 1, 2, and 3), 100 mg of each sample was transferred into separate volumetric flasks having 100 mL blend of ethanol: DW (1:1). The dispersions were subjected to bath sonication at 50 °C for 2 hours to facilitate complete leaching of curcumin from the composite matrix. Upon sonication, the solutions were filtered by using 0.45-micron membrane filters. The resulting filtrates were appropriately diluted, and absorbance was recorded at 423 nm by using UV-Visible spectrophotometer (Shimadzu UV-1900i).

Curcumin clay-composites pH Stability

There is a report that about 90% of curcumin decomposed within 30 min when incubated in pH 7.2 and the stability of curcumin was strongly improved by lowering the pH [23]. In view of this, various pH conditions were selected to evaluate whether curcumin clay composites (NCGC1) could increase the stability of curcumin, in comparison to free curcumin as a control group. A known amount of NCGC1 and free curcumin was added into a series of pH solutions (pH= 3, 6, 7, 8 and 10) with the ratio of 1:10. All samples were incubated at room temperature. Sample aliquots were collected at predetermined time intervals (0, and 30 min) and then the residual amount of curcumin was determined using UV-Visible spectrophotometer (Shimadzu UV-1900i) at 423 nm [24]. Based on the absorbance temporal variation, a curcumin degradation percent (%CD) can be defined as follows:

$$\%CD = 100\ (A0\text{-}At/\ A0) \quad \ldots\ldots\ldots\ldots\ldots\ldots (3)$$

where A0 is the initial absorbance and At is the absorbance at time t. [25]

Release of Curcumin from clay-composites

Pelletized samples of NCGC 1, 2, and 3 (250 mg each) were individually placed into 250 mL beakers containing 200 mL of phosphate buffered solution pH 5.8 and maintained at room temperature. Sample of 1 mL was withdrawn at predetermined time intervals and replaced with same volume of drug-free buffer. The collected samples were appropriately diluted, and the absorbance was measured at 423 nm using a UV-Visible spectrophotometer (Shimadzu UV-1900i) [22].

Fourier transform infrared spectroscopy analysis (FTIR)

Using a Bruker FTIR spectrophotometer, the FTIR spectra of curcumin, MT, GG, GL and NCGC1 were acquired at room temperature. Infrared spectra were analyzed using the KBr pellet technique at a resolution of 4 cm^{-1} over the 4000–400 cm^{-1}.

Scanning electron microscopy and energy dispersive X-ray analysis (SEM-EDX)

It was performed using a JEOL JSM-IT200 instrument under high vacuum conditions. Samples of MT, and NCGC1 composites were mounted on carbon stubs, followed by conductive coating to prevent charging. Imaging was carried out at an accelerating voltage of 20 kV, working distance ~11.1–11.3 mm, magnification ×500–×10,000, and field of view ~12.6 × 9.4 µm, with secondary electron detection (SED). EDX spectra were acquired using a standardless ZAF quantification method, with a live time of 30 seconds, ~1% dead time, and count rates between 258–358 CPS. [26]

Thermogravimetric Analysis (TGA)

TGA of NCGC1 clay composite was carried out on a TA Instruments SDT-Q600. Samples of 10–15 mg were placed in appropriate crucibles and heated from ambient temperature to 1000 °C at a constant heating rate of 10 °C min^{-1} under a nitrogen flow rate at 100 cm^3/min.

Differential scanning calorimetry (DSC)

A Mettler-Toledo, Switzerland was used to analyse curcumin, GL, GG, and the NCGC1 clay composite. Samples were precisely weighed into sealed aluminum pans and placed in the DSC with reference pans; the cell was equilibrated at 25 °C for 10 minutes before heating. The scan was proceeded from 25 °C to 300 °C at 10 °C/min with N_2 purging at 20mL/min.

Antimicrobial Activity

The antimicrobial activity of the curcumin clay composite NCGC1 was assessed by the agar well diffusion method against bacterial strains *Pseudomonas aeruginosa* (MTCC-424), *Staphylococcus aureus* (MTCC-96), and the fungus Candida albicans (MTCC-183). Sterile agar (15–20 mL) was poured aseptically into petri dishes to a depth of 3–4 mm. Plates were allowed to cool down, followed by refrigerated for 20 min to solidify. Culture suspension of *S. aureus* and *P. aeruginosa,* each microorganism was cultured at concentration of 1.5×10^6 separately on agar medium [27, 28]. Each plate was made with 4 agar wells using a sterile 6 mm SS borer aseptically. Similarly, Sabouraud dextrose agar (SDA) media was used for *Candida albicans.* Samples were prepared in sterilized DW to get 2.5 mg/mL concentrations of NCGC1, curcumin aqueous suspension and curcumin in DMSO (reference standard) and DMSO solvent control denoted as A, B, and D respectively, dispensed 100 µl of each into their corresponding wells.

RESULTS AND DISCUSSION

Phase solubility study

Interestingly, an increase in solubility of curcumin up to 0.776 mg/mL at 0.75 % w/v of GL was observed and further addition of GL showed non-significance in solubility [29]. As shown in Figure 1, curcumin phase solubility with GL fits an AN-type model, which corresponds to a incremental increase in solubility up to a certain extent and yields with curcumin:GL complex in a 1:9.6 ratio; the observed solubility enhancement was likely attributed to improved wetting of curcumin by GL, enabling dissolution of curcumin in the dispersed system.

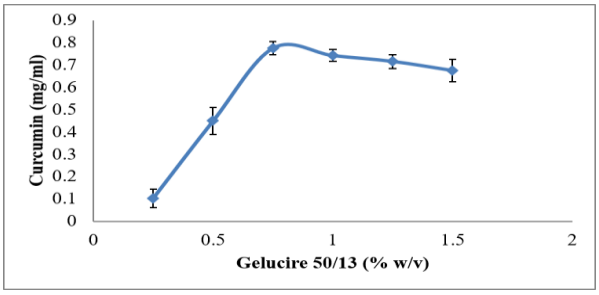

Fig. 1: Phase solubility study of curcumin in DW containing Gelucire 50/13.

The calculated Gibbs free energy (ΔG^0), a key thermodynamical parameter, exhibited increasingly negative values, indicating that the collaboration evolves into more encouraging and spontaneous. Notably, ΔG^0 values decreased further with rising GL concentrations above 0.75 % w/v, as shown in Table 2, although this trend plateaued beyond a certain threshold. Previous studies suggest that the complexation between GL and curcumin may involve Van der Waals forces, hydrophobic interactions and hydrogen bonding, collectively facilitating the formation of a solution [20]. The Ks value was found to be ≈ 1.286 suggests higher-order and stable complexation, that the curcumin and GL molecules are not just forming simple complex. Thus, study suggested that GL at 0.75% w/v was highly effective for enhancing solubility of curcumin. Solubility plateaus or drops were observed beyond 0.75% w/v of GL, may attributed to saturation or aggregation effects.

Table 2: Calculation of Gibbs free energy of curcumin.

S_1	S_0	S_0/S_1	Log	ΔG KJ/mol
0.006	0.102 ±0.041	17.10	1.231	-7.05
0.006	0.449 ±0.061	74.94	1.874	-10.46
0.006	0.776 ±0.018	129.35	2.111	-11.79
0.006	0.742 ±0.027	123.76	2.092	-11.68
0.006	0.716 ±0.031	119.40	2.077	-11.60
0.006	0.675 ±0.05	112.56	2.051	-11.45

±standard deviation (N = 3)

Conformational analysis by molecular modeling

Curcumin and GL had total potential energies of 153.25 kcal/mol and 214.15 kcal/mol, respectively, without complexations (Figure 2, A & B). The lowest-energy configuration of the drug–carrier complex supports the potential formation of a stable curcumin-GL complex. indicating favorable molecular interactions helpful to complexation. By creating two hydrogen bonds, the drug molecule was able to attach itself to the GL at the oxygen and hydrogen groups, (Figure 2, C). It has been noted that upon complexation with GL, the total potential energy of curcumin decreased to 127.75 kcal/mol. The solubility enhancement is complemented by a decline in potential energy, revealing of a more stable molecular assembly of curcumin-GL complex [21].

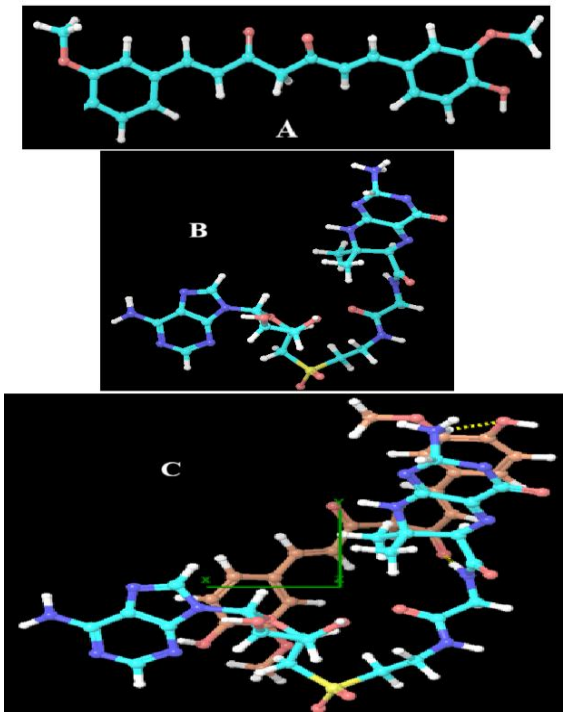

Fig. 2: Conformational analysis (A) Structure of curcumin, (B) Structure of GL,
(C) Energy minimized structure of curcumin-GL complex

Preparation dual component system of Curcumin-GL-GG- MT clay-composite

Adapted dual strategy component system by solvent dispersion and evaporation method was significant for development of clay composite with a good yield. The yellow color of curcumin changed to yellow brown upon incorporation into MT-GG. Corroborating physical integration between curcumin-GL and GG-MT. Further GG is ionic polymer that may cause electrostatic interactions with MT. The viscosity and electrokinetic properties of the system are influenced by the surface binding of GG onto the MT clay particles.

Curcumin Content estimation

The curcumin content in the clay-composite was quantified by using UV- Vis. spectroscopy. All three batches exhibited drug content in the range of 88.65–97.32% (Table 2), indicating minimal drug loss during the preparation process. The good drug content reflects the efficiency of the formulation method in retaining curcumin within the clay-composite matrix. This also revealed that solvent dispersion and evaporation method was significant with reproducible results. Minor variation in content uniformity was attributed to the intercalation of curcumin into montmorillonite (MT) layers. This was further substantiated by the increased MT content as observed in clay composites NCGC2 and NCGC3.

Table 3: Curcumin content in clay-composite

Clay-composite Code	Drug Content	
	mg	%
NCGC1	4.72 (0.16)	97.32
NCGC2	3.59 (0.18)	92.05
NCGC3	2.91 (0.12)	88.65

Values in parenthesis ±standard deviation (N = 3)

Curcumin clay-composites pH Stability

The stability of free curcumin (FC) and NCGC1 was evaluated at different pH values (3, 6, 7, 8, 10). As shown in Figure 3, curcumin degradation was strongly pH-dependent. Free curcumin degraded rapidly at neutral/alkaline pH (59.99% at pH 7; 70.16% at pH 10), while NCGC1 showed lower degradation (42.75% and 61.8%). At acidic pH 3, both were stable (FC 14.1%, NCGC1 12.2%). At mildly basic pH 8, NCGC1 resisted better (15.57%) than FC (36.98%). Overall, these results confirm that curcumin degradation is highly pH dependent, consistent with previous reports that curcumin undergoes rapid hydrolytic and oxidative

decomposition near neutral and basic pH (6). The improved stability of the NCGC1 can be attributed to the amphiphilic micellization by GL of curcumin [30]. Further GG matrix and MT interlayer adsorption providing additional stabilization.

Together, these interactions create a dual barrier system that, encapsulation by GL and physical entrapment within the GG and MT clay matrix resulting in a 10-25% improvement in curcumin stability compared to free curcumin.

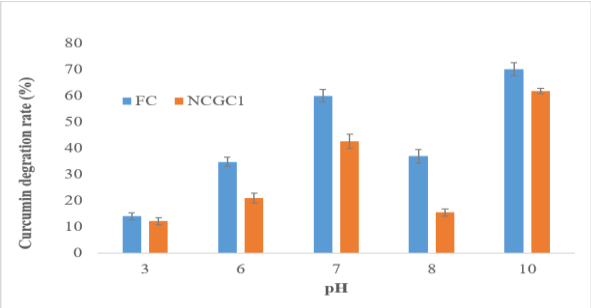

Fig. 3: Stability study of free curcumin and NCGC1 in different pH.

Release of curcumin from clay-composites

The *in vitro* curcumin release from the clay composites were assessed in phosphate buffer pH 5.8. The clay composites showed 97%, 75.14%, and 48.29% drug release at the end of 6 h for NCGC1, NCGC2 and NCGC3 respectively. Based on the drug release profile, it has been clear that as the MT and GG ratio increases from 1:1 to 3:1, the drug release was reduced. In case of NCGC1 highest release may be due to less amount of clay, and it is well evident through decreased release from NCGC2, followed by NCGC3, where clay concentration is high comparatively NCGC1. Which could be due to more surface interaction of polymer and drug with higher concentration of MT, this also demonstrated in content estimation study. Further, it was also observed that more than 50% release within 90 minutes of time interval from NCGC1 pelletized formulation, that could be synergistic effect of the GG increased swelling and GL is a lipid-based excipient with surfactant properties that improve solubility of curcumin.

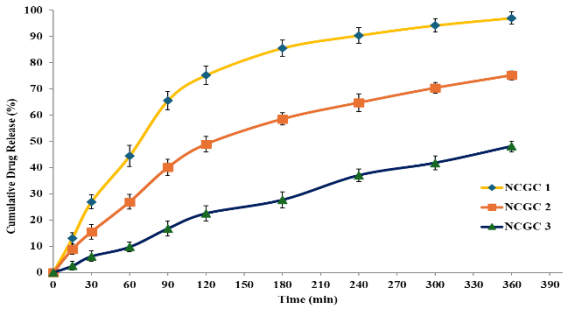

Fig. 4: *In vitro* curcumin release profile from clay-composites.

FTIR

FTIR spectrum of curcumin, MT, GG, GL, and NCGC1 clay-composite were recoded and showed in Figure 5. As per the Figure 5(a) curcumin exhibited peak with broader shift at 3375 cm^{-1} phenolic (O-H) stretching vibration, 1621cm^{-1} overlapping of carbonyl (C=O) and alkenes (C=C) stretching vibration. Aromatic (C=C) stretching vibration at 1428 cm^{-1} with 1275cm^{-1} (C-O) stretching vibration. As shown in Figure 5(b), MT exhibited a significant peak at 3624 cm^{-1}, corresponding to OH group bound with aluminum cations. Further, a peak at 3691 cm^{-1} was related to O-H stretching vibrations for octahedral cations or moisture within MT. Prominent peaks at 917 cm^{-1} Al-OH bending vibrations of in layered silicates and within the range of 1125-1177 cm^{-1} are associated with stretching vibrations (Si-O) of silica within inter layers of MT [31].

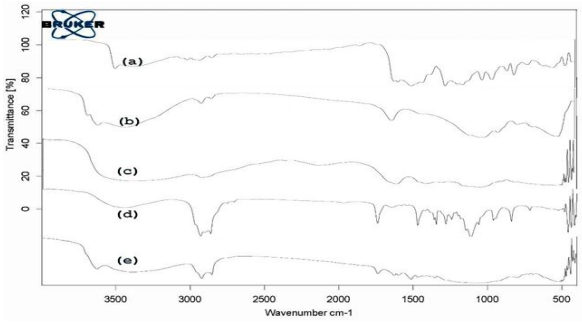

Fig. 5: FTIR spectrum of (a) curcumin, (b) MT, (c) GG, (d) GL, (e) NCGC1 clay-composite

The bands corresponding with the AlAlOH and AlMgOH bending vibrations were observed at 917 and 787 cm^{-1}, respectively. As seen in Figure 5(c), GG depicted the characteristic broadband at 3394 cm^{-1} (aliphatic alcohol) and peaks at 2922 (CH_2 group), 1049 cm^{-1} (CO stretching of hydroxyl group), 1606 and 1411 cm^{-1} (asymmetric and symmetric stretching of -COO group) and 866 cm^{-1} (C-H). As shown in Figure 5(d), GL typically displayed prominent peaks around 3420 cm^{-1} recognized to O-H stretching vibrations from the polyethylene glycol component, and a peak at 1735 cm^{-1} representing to C=O stretching vibration of the glyceride ester. As observed from Figure 5(e), for NCGC1 clay-composite, with GG- curcumin matrix encapsulated with MT layers, presented peaks for curcumin, GG, GL, and MT, affirming the occurrence of these within the clay composite. Peak widening at 3322 cm^{-1} suggested interaction with GG and hydrogen bonding atmosphere within the MT inter-gallery spacing. Whereas shift in -COO- bond of GG from 1606 to 1512 cm^{-1} accounts for the interactions of GG with curcumin and MT along with retention of peak 1736 cm^{-1} corresponding to the C=O stretching vibration of the glyceride ester group of GL. In addition to GL- curcumin, interaction of GG- curcumin matrix binding to the surface of the MT.

SEM–EDX

The SEM-EDX analysis (Figure 6 a & b) revealed a clear compositional shift upon organic incorporation in NCGC1, where the aluminosilicate profile of MT (O 54.94%, Si 36.14%, Al 7.92%) was transformed into a carbon-rich matrix (C 47.64%, O 38.68%) with suppressed silicon (10.50%) and aluminum (2.52%). Morphologically, SEM images distinguished the plate-like surfaces of MT from the homogenized texture of NCGC1, confirming successful curcumin and GL loading. The strong carbon and oxygen peaks highlight the dominance of organic components, while residual silicon and aluminum signals indicate the persistence of the clay framework. These findings support the role of gellan gum in mediating MT interactions through cation bridging (Li^+, Na^+, Ca^{2+}) and hydrogen bonding between gellan hydroxyl groups and MT siloxane oxygens, thereby stabilizing the composite structure [32].

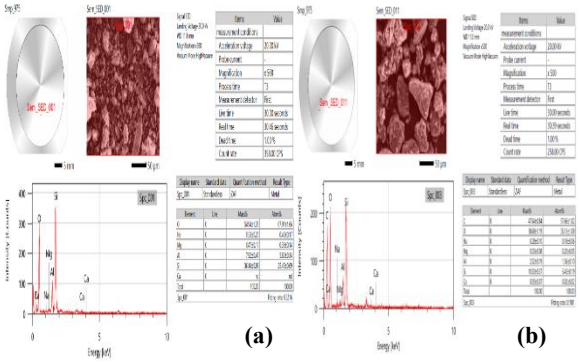

Fig. 6: SEM-EDX of NCGC1 clay-composite (a) and MT (b)

Thermogravimetric analysis

TGA analysis for clay composites was shown in Figure 7. A weight loss of 2.993%, arround 60 °C suggests evaporation of surface and interlayer water from MT or decomposition of low-melting excipients like GL. The second event near 291 and 334 °C with 11.84% weight loss indicate onset of curcumin degradation, especially if complexed or dispersed in a matrix of GG. The major weight loss of 14.58 % between 613–656 °C reflects complete breakdown of organic matter, including curcumin, GL and GG polymeric carriers. The high residual mass of 64.64% at 956 °C confirms the presence of thermally stable inorganic components, likely aluminosilicate sheets of the MT, which do not decompose at these temperatures, and this could be also contributed to collapsing of the clay layers.

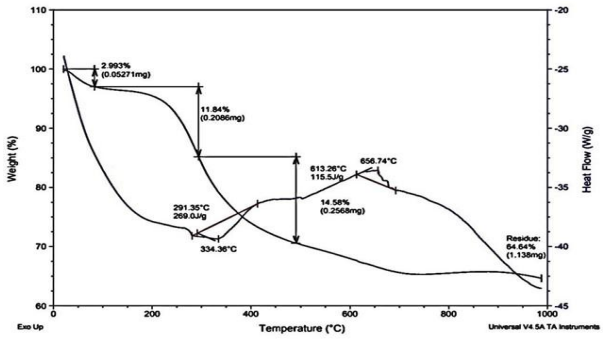

Fig. 7: Thermogravimetric analysis of NCGC1.

Differential scanning calorimeter

The DSC thermograms of pure curcumin, Gelucire 50/13 (GL), gellan gum (GG), and the clay nanocomposite formulation (NCGC1) are illustrated in Figure 8. Pure crystalline curcumin exhibited a sharp, well-defined endothermic melting peak at 184.30 °C with an enthalpy of

fusion at 68.62 J/g, confirming its highly ordered crystalline nature (Figure 8a). In contrast, the thermogram of the nanocomposite formulation (NCGC1) showed a highly suppressed, broad endothermic event at 166.97 °C, with the enthalpy dropping drastically from 68.62 J/g to 11.52 J/g (Figure 8d). This significant reduction in enthalpy and peak broadening confirms that a major fraction of curcumin underwent a transition from a crystalline state to a high-energy amorphous solid state or molecular dispersion within the matrix.

Pure GL exhibited its characteristic lipid melting endotherm at 43.79 °C (Figure 8b), which shifted slightly upward to 48.63 °C in the NCGC1 composite matrix (Figure 8d). This shift indicates strong hydrophobic and spatial interactions during the molecular dispersion of curcumin within the lipid carrier. For raw GG (Figure 8c), two characteristic thermal transitions were observed: a broad desolvation loop at 65.62 °C (associated with moisture loss) and a sharp polymer degradation/melting peak at 249.23 °C. In the NCGC1 composite (Figure 8d), these peaks shifted to 58.48 °C and 251.99 °C, respectively. The elevated polymer degradation temperature (251.99 °C) directly indicates restricted polymer chain mobility, arising from strong intermolecular hydrogen bonding and successful intercalation within the MT clay layers.

Taken together, these DSC thermal profiles confirm the homogeneous molecular dispersion of curcumin, its complete amorphization by the GL carrier, and its successful encapsulation within the protective NCGC1 clay composite architecture.

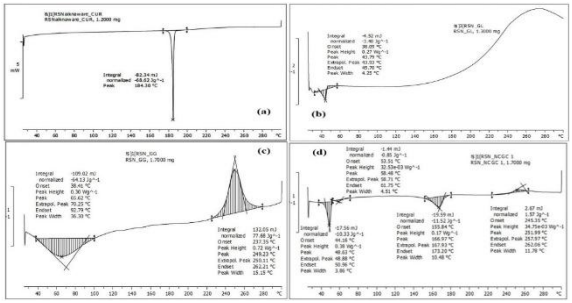

Fig. 8: DSC thermogram of curcumin (a), GL (b), GG (c) and NCGC1 (d)

Antimicrobial activity of clay-composite

Antimicrobial potential of, curcumin in DMSO, curcumin aqueous suspension, and control DMSO results are shown in Figure 9. *Pseudomonas aeruginosa* (MTCC 424), *Staphylococcus aureus* (MTCC 96) bacterial strains were used, and *Candida albicans* (MTCC 183) as a fungal strain by the Agar well diffusion method. These microorganisms only were selected as these commonly involved in skin infections like Boils, abscesses, cellulitis, wound infections, Candidiasis, etc. The curcumin clay-composite (NCGC 1) in aqueous medium showed a 10, 13 and 12 mm zone of inhibition against *Pseudomonas aeruginosa, Staphylococcus aureus* and *Candida albicans,* respectively Figure 9 (A). Whereas comparatively curcumin in DMSO showed 14, 15 and 13 mm respectively against these strains Figure 9 (B). Curcumin exhibited marginally enhanced efficacy in DMSO, that was due to high solubility of curcumin in DMSO solvent. Interestingly, the curcumin aqueous suspension, when tested against both bacterial and fungal strains, did not exhibit significant

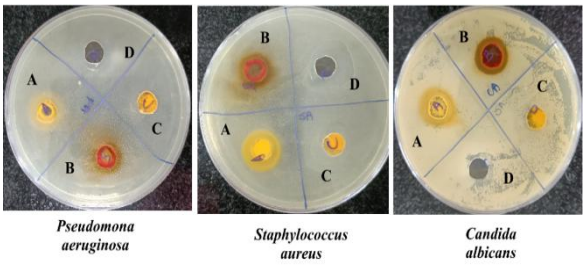

Fig. 9: Antimicrobial potential of (A), curcumin in DMSO (B), curcumin aqueous suspension (C) and DMSO (D)

inhibitory effects Figure 9 (C). This lack of activity is likely attributable to poor aqueous solubility of curcumin in the present adopted study condition [33]. DMSO as solvent also did not elicit any notable response against all microorganisms Figure 9 (D). A decisive remark was drawn from antimicrobial activity, that the substantial effect was due to improved solubility and dissolution of curcumin within aqueous phase.

CONCLUSION

As supported by the observations of the characterizations, polyoxylglycerides based clay composite for promoting solubility, stability and antimicrobial potential of curcumin were efficiently developed. In concern to GL, GG and MT ratio or type noticeably influenced the curcumin solubility and dissolution profile. Optimized clay composite NCGC1 exhibited higher solubility, stability and dissolution with all desired physicochemical characterization with significant results. It was collectively revealed in curcumin antimicrobial activity that to be in aqueous phase, affirmed potentials of curcumin against tested strains of bacteria and fungus. Dual strategy of polyoxylglycerides tailored with swellable polymer clay composite system is also useful and straightforward. Which offered a viable alternative to other poorly soluble therapeutic agents exhibiting physicochemical traits like curcumin. This platform can be utilized for both oral and topical routes of administration with added benefits of biocompatible inactive components, offering great formulation flexibility.

REFERENCES

1. Gornicka J, Mika M, Wroblewska O, Siudem P, Paradowska K. Methods to improve the solubility of curcumin from turmeric. Life. 2023;13(1):207.
2. Pulido-Moran M, et al. Curcumin and health. Molecules. 2016;21(3):264.
3. Negi PS, Jayaprakasha GK, Rao LJ, Sakariah KK. Antibacterial activity of turmeric oil: a byproduct from curcumin manufacture. J Agric Food Chem. 1999;47(10):4297–300.
4. Rathore S, Mukim M, Sharma P, Devi S, Nagar JC, Khalid M. Curcumin: a review for health benefits. Int J Res Rev. 2020;7(1):273–290.
5. Anand P, Kunnumakkara AB, Newman RA, Aggarwal BB. Bioavailability of curcumin: problems and promises. Mol Pharm. 2007;4(6):807–818.
6. Wang YJ, Pan MH, Cheng AL, Lin LI, Ho YS, Hsieh CY, et al. Stability of curcumin in buffer solutions and characterization of its degradation products. J Agric Food Chem. 1997;45(7):2574–2578.
7. Gordon ON, Luis PB, Schneider C. Autooxidation of curcumin provides a bifunctional compound with antioxidant and anti-inflammatory activity. J Biol Chem. 2015;290(8):4817–4828.
8. Adhikari L, Kumar N, Saha A, Semalty A, Semalty M. Curcumin nanoparticles: exploring types and their impact on bioavailability, permeability, and solubility. Micro Nanosyst. 2025;17(1):e211024.
9. Cheng C, Peng S, Li Z, Zou L, Liu W, Liu C. Improved bioavailability of curcumin in liposomes prepared by a pH-driven method. RSC Adv. 2017;7(42):25978–25986.
10. Schiborr C, Kocher A, Behnam D, Jandasek J, Toelstede S, Frank J. The oral bioavailability of curcumin from micronized powder and liquid micelles is significantly increased in healthy humans and differs between sexes. Mol Nutr Food Res. 2014;58(3):516–527.
11. Tejada S, Manconi M, Manca M, Marongiu F, Miralles A, Capó X, et al. Polymeric nanoparticles for increasing oral bioavailability of curcumin. Antioxidants (Basel). 2018;7(4):46.
12. Bertoni S, Albertini B, Ferraro L, Beggiato S, Dalpiaz A, Passerini N. Exploring the use of spray congealing to produce solid dispersions with enhanced indomethacin bioavailability: in vitro characterization and in vivo study. Eur J Pharm Biopharm. 2019;139:132–141.
13. Bertoni S, Albertini B, Passerini N. Different BCS class II drug–Gelucire solid dispersions prepared by spray congealing: evaluation of solid state properties and in vitro performances. Pharmaceutics. 2020;12(6):548.
14. Qi S, Marchaud D, Craig DQM. An investigation into the mechanism of dissolution rate enhancement of poorly water-soluble drugs from spray-chilled Gelucire 50/13 microspheres. J Pharm Sci. 2010;99:262–274.
15. Panigrahi KC, Patra CN, Jena GK, Ghose D, Jena J, Panda SK, Sahu M. Gelucire: a versatile polymer for modified release drug delivery system. Future J Pharm Sci. 2018;4:102–108.
16. BenchChem. Stability of curcumin in different pH and temperature conditions. 2024. https://pdf.benchchem.com/1669/Stability_of_curcumin_in_different_pH_and_temperature_conditions.pdf
17. Abu Elella MH, Khutoryanskiy VV. Gellan gum in drug delivery. In: Nayak AK, Hasnain MS, Aminabhavi TM, editors. Natural Biopolymers for Drug Delivery. Woodhead Publishing Series in Biomaterials. London: Woodhead Publishing; 2025. 339-360. doi:10.1016/B978-0-323-95367-2.00024-7.
18. Asif AH, Asha BR, Prasanthi S, Goudanavar P, Prashantha K, Srikruthi KS, et al. Montmorillonite in next-generation drug delivery: patent trends, safety insights, and industrial advancements. J Mater Sci Mater Med. 2026. doi:10.1007/s10856-026-07031-4.
19. Higuchi T, Connors KA. Phase-solubility techniques. Adv. Anal. Chem. Instrum. 1965;4, 117–212.
20. Hanif M, Khan R, Bano S, et al. Improved solubility and corneal permeation of PEGylated curcumin complex used for the treatment of ophthalmic bacterial infections. PLoS One. 2022;17(3):e0266654. doi:10.1371/journal.pone.0266654

21. Jammula S, Patra CN, Swain S, Panigrahi KC, Patro AP, Beg S, Dinda SC, Rao MEB. Improvement in the dissolution rate and tableting properties of cefuroxime axetil by melt-granulated dispersion and surface adsorption. Acta Pharm Sin B.2013;3(2):113-22. doi:10.1016/j.apsb.2013.01.001
22. Madusanka N, de Silva KM, Amaratunga G. A curcumin activated carboxymethyl cellulose-MT clay composite having enhanced curcumin release in aqueous media. Carbohydr Polym. 2015;134:695-9. doi:10.1016/j.carbpol.2015.08.030
23. Wang YJ, Pan MH, Cheng AL, Lin LI, Ho YS, Hsieh CY, Lin JK. Stability of curcumin in buffer solutions and characterization of its degradation products. J Pharm Biomed Anal. 1997;15(12):1867-76.
24. Chen X, Zou LQ, Niu J, Liu W, Peng SF, Liu CM. The stability, sustained release and cellular antioxidant activity of curcumin nanoliposomes. Molecules. 2015;20(8):14293-311. doi:10.3390/molecules200814293
25. Martínez-Guerra J, Palomar-Pardavé M, Romero-Romo M, Ramírez-Silva MT, Palomar-Pardavé M. New insights on the chemical stability of curcumin in aqueous media at different pH: Influence of the experimental conditions. Int J Electrochem Sci. 2019;14:5373-85. doi:10.20964/2019.06.24
26. Derungs I, Rico M, Lopez J, Barral L, Montero B, Bouza R. Influence of the hydrophilicity of montmorillonite on structure and properties of thermoplastic wheat starch/montmorillonite bionanocomposites. Polym Adv Technol. 2021;32(12):4479-89. doi:10.1002/pat.5450
27. Farrokhi H, Koosha M, Nasirizadeh N, Salari M, Abdouss M, Li T, Gong Y. The effect of nanoclay type on the mechanical properties and antibacterial activity of chitosan/PVA clay-composite films. J Compos Sci. 2024;8(4):255. doi:10.3390/jcs8040255
28. Valgas C, Souza SM, Smânia EFA, Smânia Jr A. Screening methods to determine antibacterial activity of natural products. Braz J Microbiol. 2007;38(2):369-80. doi:10.1590/S1517-83822007000200034
29. Mohamed JM, Kavitha K, Karthikeyini S, Chitra S, Nandhineeswari S. Soluble curcumin prepared by solid dispersion using four different carriers: Phase solubility, molecular modelling and physicochemical characterization. Trop J Pharm Res. 2019;18(8):1581-8.
30. Shinde UK, Suryawanshi DG, Amin PD. Development of Gelucire® 48/16 and TPGS mixed micelles and its pellet formulation by extrusion spheronization technique for dissolution rate enhancement of curcumin. AAPS PharmSciTech. 2021;22(5):182. doi:10.1208/s12249-021-02032-8. PMID:34129146
31. Caccamo MT, Mavilia G, Mavilia L, Lombardo D, Magazù S. Self-assembly processes in hydrated montmorillonite by FTIR investigations. Materials (Basel). 2020;13(5):1100. doi:10.3390/ma13051100. PMID:32121630; PMCID:PMC7084999
32. Caliman WR, Sentanin FC, Sabadini RC, Garcia RHS, Monaretto T, Colnago LA, Pawlicka A. Gellan gum-montmorillonite nanocomposites for electrochromic devices. Coatings. 2023;13(2):350. doi:10.3390/coatings13020350
33. Ratrey P, Dalvi SV, Mishra A. Enhancing aqueous solubility and antibacterial activity of curcumin by complexing with cell-penetrating octaarginine. ACS Omega. 2020;5(30):19004-13. doi:10.1021/acsomega.0c02321